## Supplementary

### S1. Results averaged by section

Table S1. Results Table by section (depth)

Rock Eval 7S - Mean ± SE

| **Section** | **Depth** | **SOC** | **R-index** | **I-index** | **Oxygen Index** | **H- index** | **TpkS2** | **PARTYsoc stable SOC** | **N** |
|---|---|---|---|---|---|---|---|---|---|
| Units | [cm] | wt.% | [Unitless] | [Unitless] | mg $CO_2$ gr-$SOC^{-1}$ | mg HC gr-$SOC^{-1}$ | °C | fraction | |
| Drained | 30-100 | 13 ±1 | 0.67 ±0.01 | -0.03 ±0.01 | 195 ±7 | 133 ±7 | 460 ±5 | 0.5 ±0.3 | **25** |
| Rewetted | 110-170* | 20 ±2 | 0.59 ±0.01 | 0.1 ±0.02 | 160 ±11 | 151±10 | 431 ±7 | 0.42 ±0.4 | **10** |
| Pristine | 200-400 | 35 ±1 | 0.49 ±0.01 | 0.26 ±0.01 | 100 ±7 | 189 ±6 | 378 ±5 | 0.38 ±0.3 | **26** |

Experimental respiration Results - Mean ± SE

| **Section** | **Depth** | **$CO_2$ Flux 22°C** | **$O_2$ Flux 22°C** | **$CO_2$ Flux 33°C** | **$O_2$ Flux 33°C** | **ARQ 22°C** | **ARQ 33°C** | **Q10 (O2)** | **N** |
|---|---|---|---|---|---|---|---|---|---|
| Units | [cm] | µmol $grC^{-1}$ $day^{-1}$ | µmol $grC^{-1}$ $day^{-1}$ | µmol $grC^{-1}$ $day^{-1}$ | µmol $grC^{-1}$ $day^{-1}$ | | | | |
| Drained | 30-100 | 9 ± 2 | -16 ±3 | 23 ±5 | -43 ±7 | 0.59 ±0.05 | 0.52 ±0.07 | 2.9 ± 0.3 | **8** |
| Rewetted | 110-170* | 16 ±2 | -37 ±4 | 40 ±7 | -104 ±11 | 0.43 ±0.07 | 0.4 ±0.1 | 2.5 ±0.4 | **4** |
| Pristine | 200-400 | 9 ±1 | -20 ±2 | 23 ±4 | -54 ±6 | 0.45 ±0.04 | 0.42 ±0.06 | 2.5 ±0.3 | **12** |

### S2. Statistical analysis

Table S2. Statistical tests - P values for significant difference

| **Section** | **SOC $^{T}$** | **R-index $^{T}$** | **I-index $^{S}$** | **Oxygen Index $^{S}$** | **H-index $^{T}$** | **TpkS2 $^{S}$** | **PARTYsoc stable SOC$^{T}$** |
|---|---|---|---|---|---|---|---|
| Drained vs Pristine | <0.0001 | <0.0001 | <0.0001 | <0.0001 | <0.0001 | <0.0001 | 0.003 |
| Rewetted vs Pristine | <0.0001 | <0.0001 | <0.0001 | <0.0001 | 0.007 | 0.0003 | ND |
| Drained vs Rewetted | 0.0016 | <0.0001 | 0.0016 | ND | ND | 0.002 | ND |
| **Section** | **$CO_2$ Flux $^{T}$ (22°C)** | **$O_2$ Flux $^{T}$ (22°C)** | **$CO_2$ Flux $^{W}$ (33°C)** | **$O_2$ Flux $^{T}$ (33°C)** | **ARQ $^{W}$ (22°C + 33°C)** | **Q10 $^{W}$ (CO2 + O2)** | |
| Drained vs Pristine | ND | ND | ND | ND | ND | ND | |
| Rewetted vs Pristine | 0.02 | 0.005 | ND | 0.0016 | ND | ND | |
| Drained vs Rewetted | 0.03 | 0.001 | ND | 0.0003 | ND | ND | |

***** $^{T}$ for Tukey-Kramer test, $^{W}$ for Welch's test, $^{S}$ for Steel-Dwass test. ND for no significant difference between the sections.

## S3. Two-pool model RMSD

As described in the material and method section, the two-pool model includes two unknown variables (see Eq. 5). The root mean square deviation (RMSD) serves as a simple objective function, where smaller values indicate a better fit to the observed data. In the RMSD contour plot, the minimum value (blue areas) represents the optimal values for the two variables, while yellow areas indicate high RMSD values corresponding to poor fits. From the resulting plot, we observe a linkage between the two variables. When the model is presented with high $SOM_P$, a high reaction constant (*k*) is required for a better fit, and vice versa. This linkage results in one optimal local minimum. To account for uncertainty, we defined a range of possible values for the two unknown variables, represented by a gray envelope. This envelope includes all combinations of variable values that result in an RMSD lower than 2.2% SOM, as this threshold captures all observed data, and it is presented in Figure 7.

.

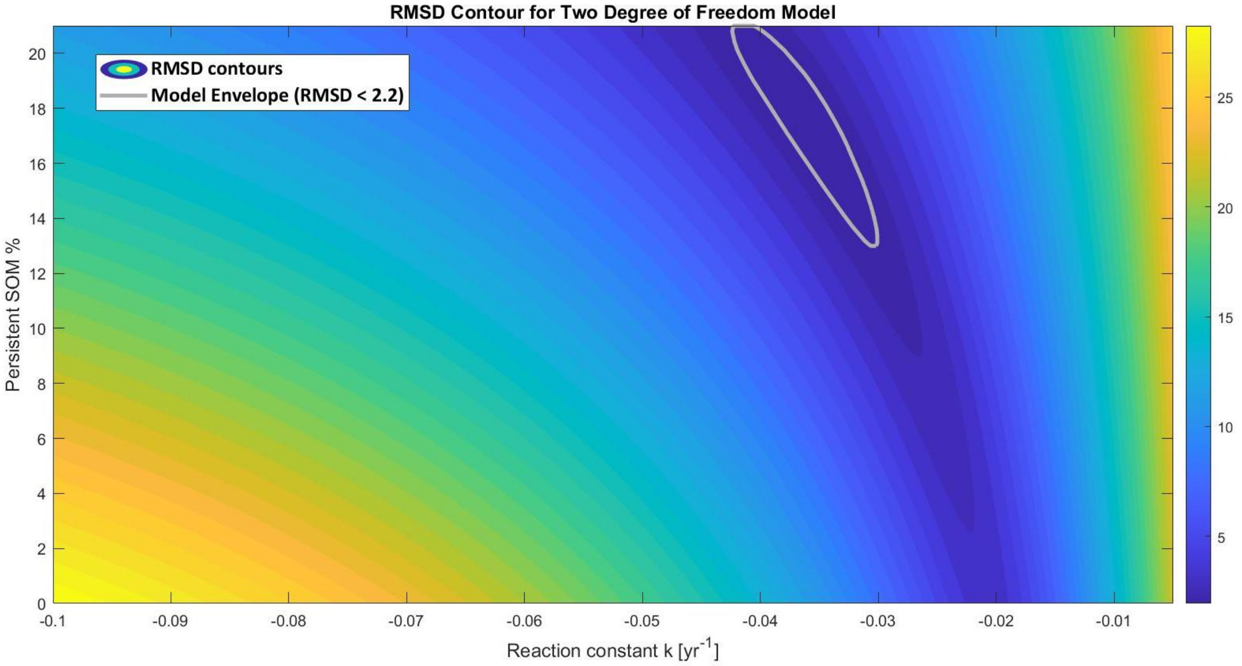

**Figure S1**: RMSD values contour and color map plot of the two unknown variables in the fitted model.

## S4. Log profiles

### Profile A

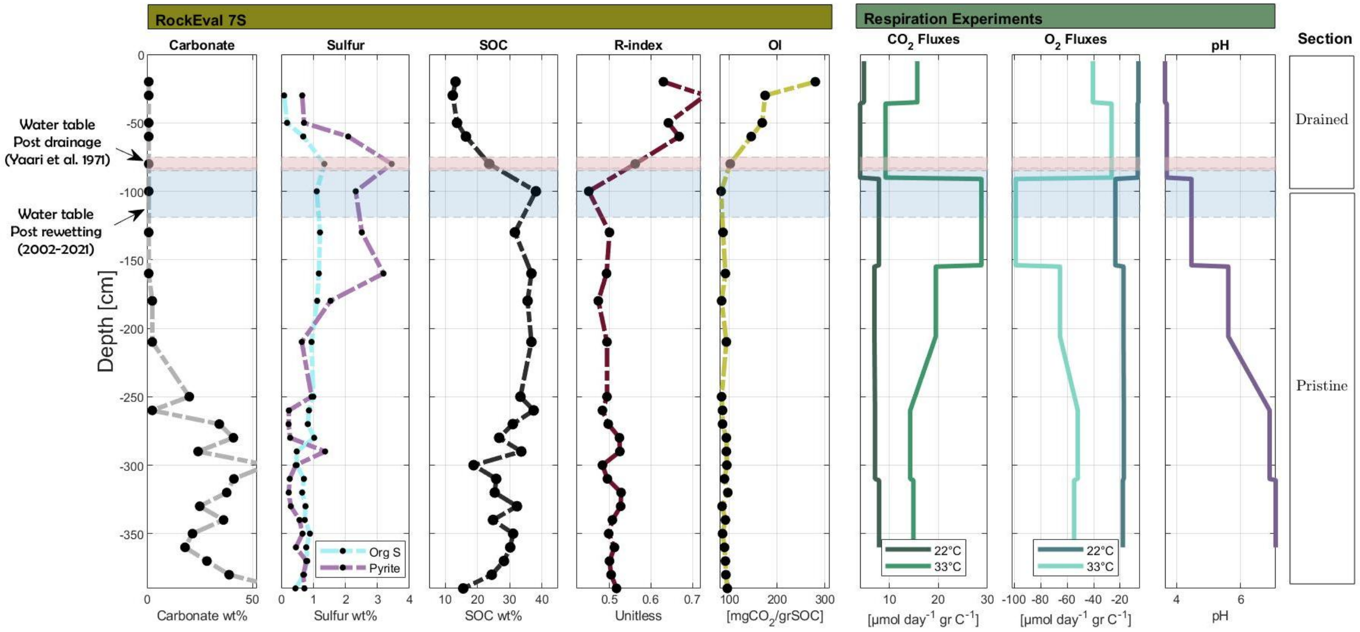

### Profile C

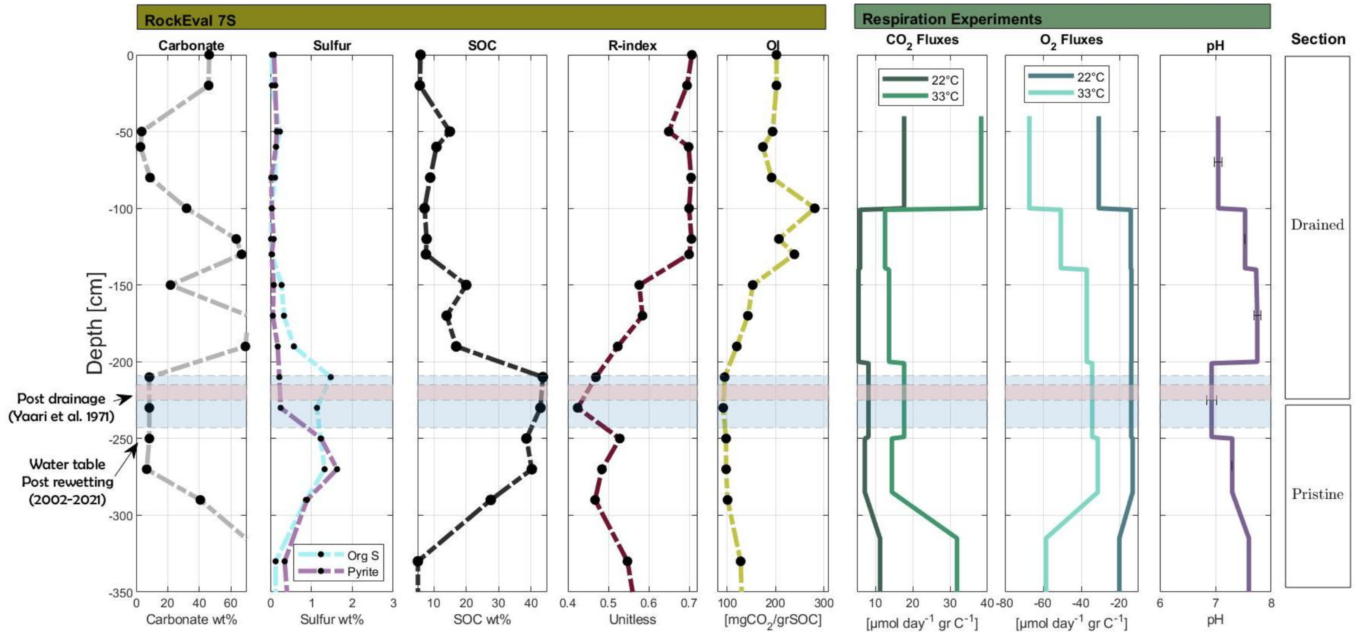

Profile E

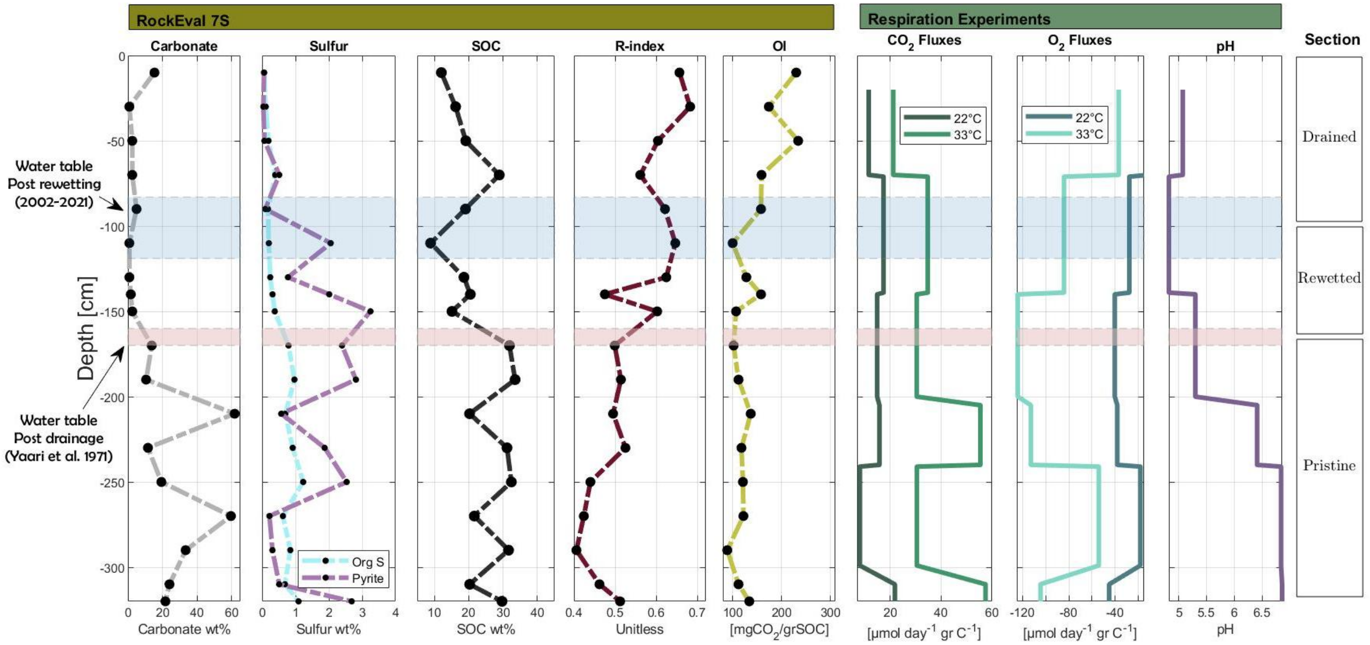

Profile D

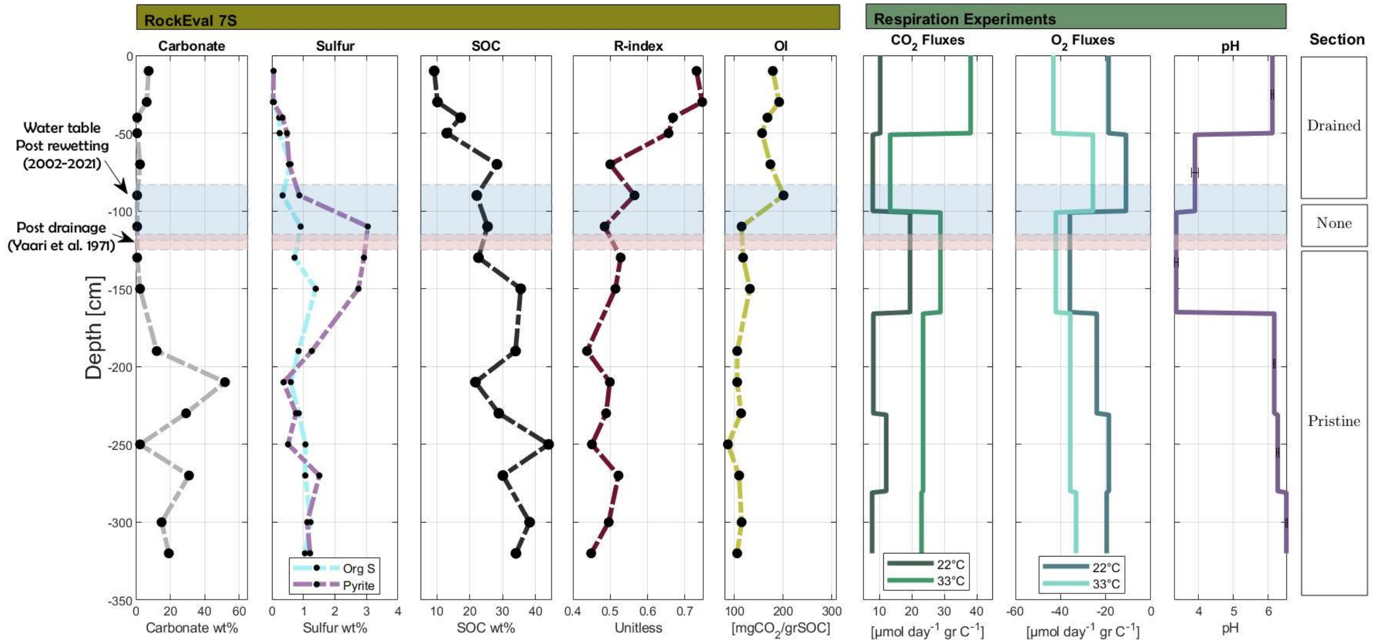

**Figure S2**: detailed log profiles A, C, E and D – left to right: Carbonate in grey; Sulfur spices; SOC in black; R-index in red; Oxygen index in yellow; $CO_2$ fluxes at 22°C and 33°C; $O_2$ fluxes at 22°C and 33°C; pH in purple. The sections are divided by the WTL's and illustrated to the right.

## S5. Loss on ignition

We have employed the Loss on Ignition (LOI) method for three main purposes: (1) evaluate soil organic matter (SOM) from soil organic carbon (SOC) measurements; (2) to examine the boundary between SOC and mineral carbon in peat samples, as Rock-Eval is primarily used for rocks and mineral soils. ; and (3) to assess changes in the carbon fraction of SOM across peat sections, since decomposition is expected to alter it.

To address these objectives, 27 samples representing all sections were finely grounded and oven-dried at 105°C overnight. Approximately 1 g of each sample was then weighed, combusted at 400°C for 16 hours, and reweighed. We selected the 400°C method, as recommended by Nelson and Sommers (1996), to minimize bias caused by structural water release from clays, which is known to occur at temperatures exceeding 350-400°C (Hoogsteen et al., 2015). Additional bias may arise from the structural water of gypsum, which begins to dehydrate at temperatures above 40°C. Given the high clay and gypsum content in Hula's degraded samples *(Yaari et al., 1971a)*, a low-temperature LOI procedure was necessary. However, despite this adjustment, some bias remains unavoidable. Furthermore, we applied post-LOI analysis using RE-7S to determine if organic carbon had fully decomposed during the LOI procedure, and to determine the thermal boundary between the release of organic carbon and mineral carbon in those peat samples.

Figure S3 shows the correlation between the LOI and the SOC by RE-7S, presented both for the pristine and degraded peat samples, in blue and red, respectively. The regression slope between LOI and SOC was determined to be 1.8 (n=9, $R^2$=0.90) for pristine samples and 1.6 (n=11, $R^2$=0.96) for drained samples, while the pristine samples have a negative intercept value, and the drained samples have a positive. Our understanding is that the intercept is caused by a bias produced by structural water in the drained samples. This bias was minimized by the 400°C LOI procedure but studies have shown that clay mineral can release structural water beneath 400°C (Hoogsteen et al., 2015). Since this bias in not very high, we choose to exclude it from the regression equation and use only the slope.

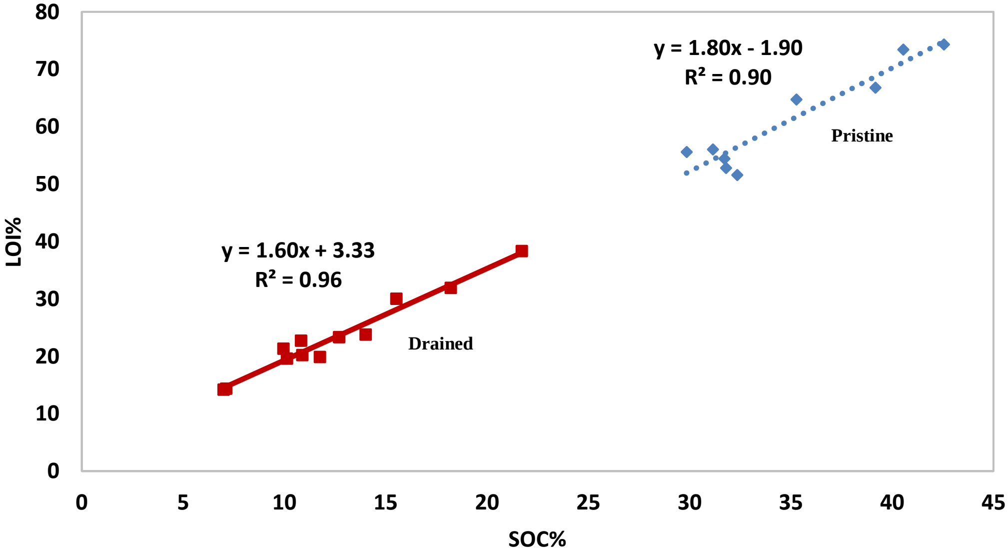

**Figure S3**: Correlation between LOI at 400C and SOC values by RE-7S. Drained (red) and Pristine (Blue) regression is separated.

Post-LOI analysis using the RE-7S confirmed that organic matter in degraded peat samples was fully decomposed at 400°C. However, in OM-rich samples, 1–2% of SOC remained, necessitating a correction. This correction was applied by subtracting the carbon content remaining post-LOI from the original carbon value. While this adjustment minimizes the error, it likely introduces a minor offset, as other components of the remaining organic carbon may also have been released. Notably, this error is relatively small and is confined to pristine samples.

By adopting the 400°C method, we effectively minimized the influence of structural water release and achieved a reliable distinction between organic and mineral carbon in the peat samples. This approach facilitates a more accurate assessment of carbon dynamics across the sections.

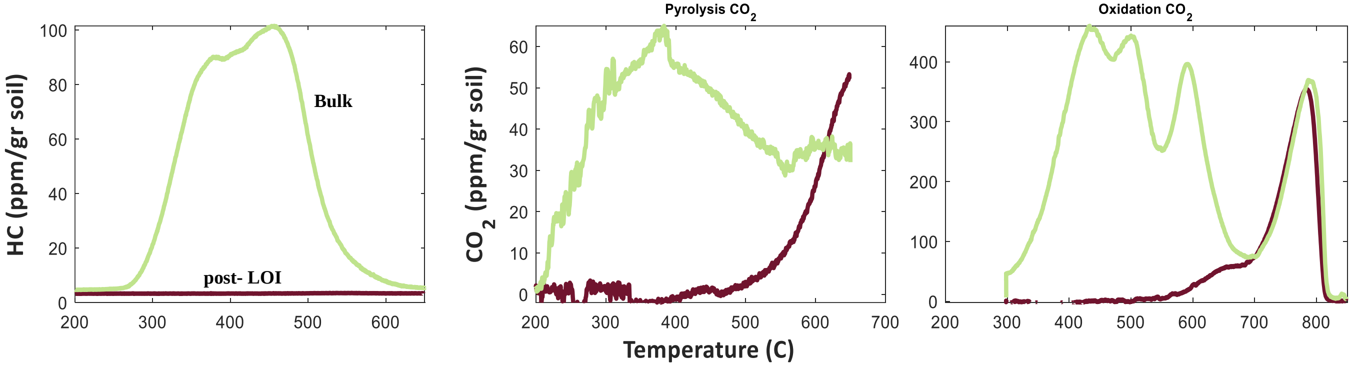

**Figure S4**: HC and $CO_2$, both from pyrolysis and oxidation phases, curves of a selected drained sample from -70 cm depth. Bulk analysis represented in green and post-LOI in red.

In Figure S4, the green line represents the bulk analysis, which accounts for both SOC and mineral carbon, while the red line represents the post-LOI analysis, reflecting the same sample after the removal of organic carbon. Pyrolysis $CO_2$ data reveal an overlap between these carbon types, where inorganic carbon begins significant release above 500°C, while organic carbon ceases release beyond 600°C. Together, these results highlight the challenge of defining a clear boundary between organic and inorganic carbon during $CO_2$ release. Consequently, the true boundary between organic and inorganic carbon likely falls between 500°C and 600°C. For our peat samples, 550°C could be a more accurate boundary. However, to maintain consistency with existing studies, we retain the 400°C boundary established by Behar et al. (2001). Notably, $CO_2$ released between 400°C and 550°C accounts for approximately 4% of total SOC in drained (mineral soil) samples and 2% in pristine samples. While this introduces a non-negligible error in SOC estimations, its impact on OI values is even more pronounced.

## S6. The PARTYsoc model

This model, in its v2.0 version we use, accounts for a wide range of data produced by RockEval and its indices, such as gases released in given temperature intervals, mineral carbon, HI, RI, I-index, OI, among others (see Cécillon et al., 2021). Unlike the thermal indices (RI and I-index), we found only a weak relationship between the persistent SOC predicted by the PARTYsoc v2.0 model and the SOC or RI values (Fig. S5). The PARTYsoc v2.0 model estimates that a fraction of 0.3 to 0.6 of the SOC is stable across all peat sections, regardless of their degradation stage. The model estimate of the stable fraction was multiplied by the SOC content, yielding a mean persistent SOC of 13.2 ± 0.8 wt.% in the pristine section and 6.1 ± 0.5 wt.% in the drained section.  Thus, implying that degraded peat contains less stable SOC than pristine peat. However, persistent SOC is not expected to decline so fast during 66 years of peat decomposition, suggesting a discrepancy in these results. One possible explanation for this discrepancy is that the PARTYsoc v2.0 model was developed and calibrated using Bare Fallow soil samples (Cécillon et al., 2021), which are low in organic carbon (3-1 wt.%). It may result in falsely evaluating some of the pristine organic carbon as persistent. As a result, the model may require further adjustments to accurately assess peat samples, which have substantially different organic characteristics.

## S7. Correlation plots

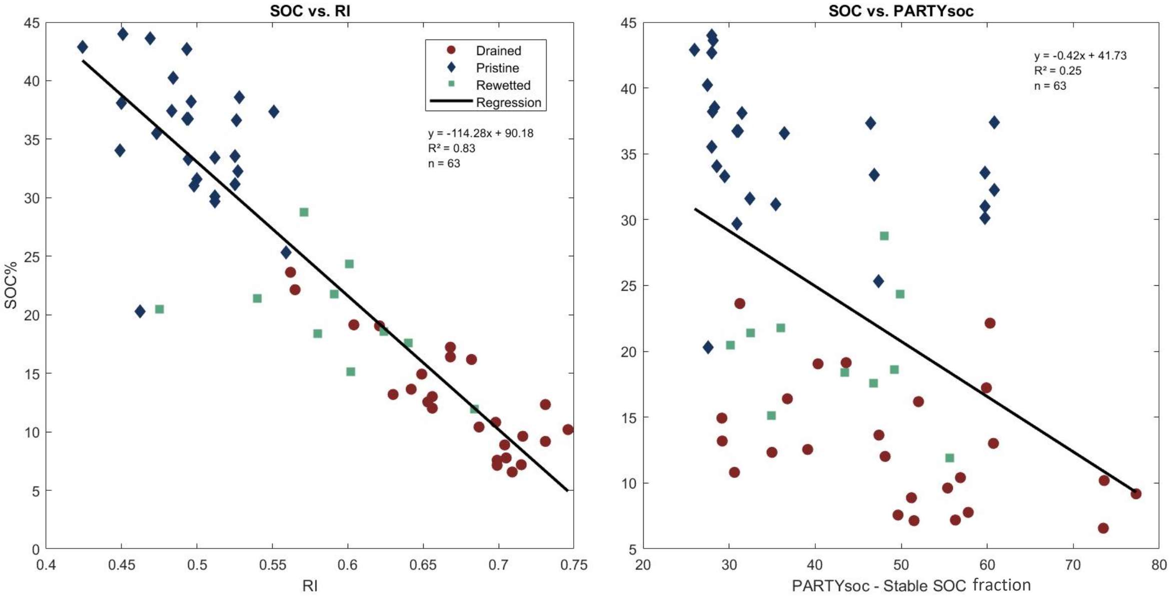

SOC vs. RI

SOC vs. PARTYsoc

**Figure S5**: SOC as function of R-index (left) and Stable fraction by the PARTYsoc (right).

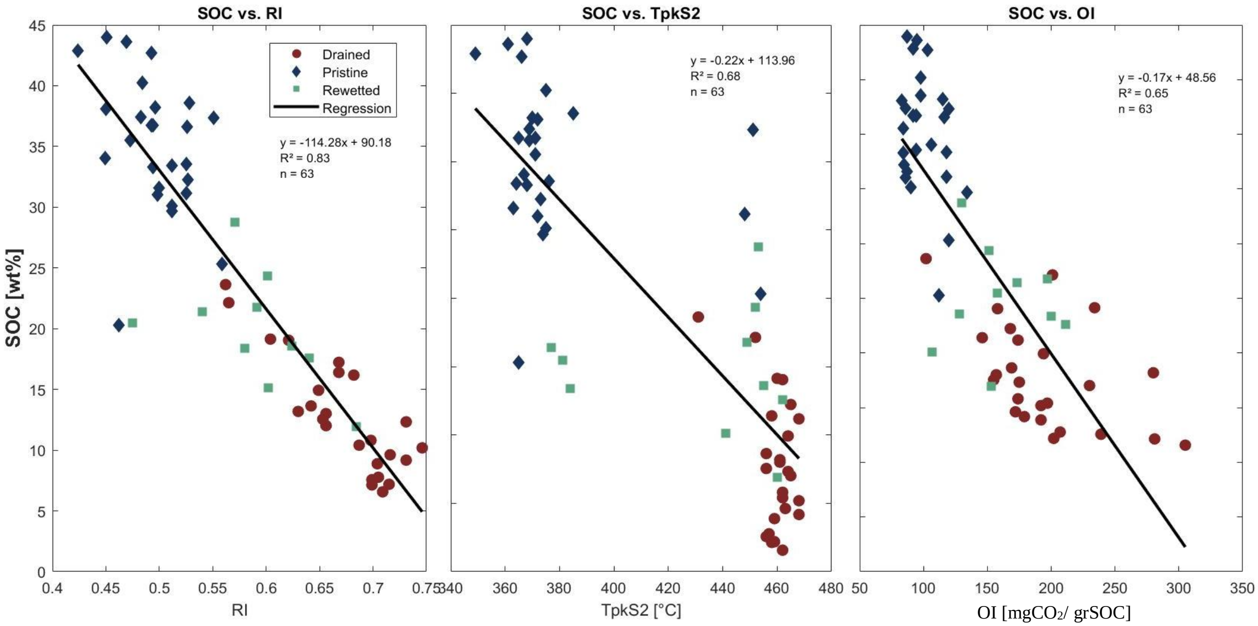

**Figure S6**: SOC as a function of R-index (RI, left), HC temperature peak (TpkS2, middle), and Oxygen Index (OI, right). Linear regression is presented in black, with results classified using a color scheme for their respective section.

## S8. Cores Location

Coordinates:

| | WGS84 | | Israel ITM | |
|---|---|---|---|---|
| Profile | Y (latitude) | X (longitude) | Y (latitude) | X (longitude) |
| A | 33.114725 | 35.6001496 | 256389 | 780009 |
| C | 33.115093 | 35.589576 | 255392 | 780048 |
| D | 33.1144424 | 35.6110686 | 257408 | 779986 |
| E | 33.1149376 | 35.6164304 | 257909 | 780037 |
| F | 33.1147508 | 35.6222117 | 258448 | 780020 |

### S9. Sulfur measurements by Rock-Eval 7S

Sulfur measurements using the RE-7S method provide a novel approach to quantifying the sulfur species. Cohen-Sadon et al. (2022) identified a correlation between the temperature of maximum organic S generation during pyrolysis (Tmax-S) and the proportion of organic S released during this phase in rock samples. The lower the peak temperatures, the higher the proportion of sulfur released in this phase. In the Hula peat samples, the organic sulfur peak occurs at an average of ~345°C, significantly lower than in rocks (above 400°C). Based on this, we assume that all organic sulfur in our peat samples is released during the pyrolysis phase, enabling a clear distinction between organic and pyrite sulfur. Sulfur species were temperature separated as follows: Organic S (pyrolysis from 200°C to a local minimum at approximately 500°C), Pyrite S (pyrolysis from ~500°C to 650°C; oxidation from 300°C to a local minimum at approximately 1000°C), and Sulfate S (oxidation from ~1000°C to 1200°C).